THE SYNERGISTIC USE OF REMOTELY SENSED DATA FOR THE DETECTION OF UNDERGROUND COAL FIRES

John L. van Genderen, Craig J.S. Cassells, Zhang Xiangmin
ITC, PO Box 6, 7500 AA, Enschede, The Netherlands

Commission VII, Working Group 7

KEY WORDS: Geology, Environment, Pollution, Monitoring, Thermal Modeling, Coal Fires

ABSTRACT

Underground coal fires are a serious problem in many parts of the world but probably the most serious occurrence of such fires at the moment is in China. Coal fires are to be found mainly in the north of the country spread out over a total distance of 5000 km east-to-west and 450 km north-to-south. The problems caused by these fires include the loss of a valuable economic resource, danger to mine workers and mining equipment, and serious environmental pollution at both local and global scales.
Extensive fire-fighting efforts are being undertaken by the Chinese Ministry of Coal Industry; however, their work is often made difficult by the remoteness of the fires. Fires are often out of control before the authorities are aware that there is a problem.
Because of this, the Aerophotogrammetry and Remote Sensing Corporation of China Coal (ARSC) and the International Institute for Aerospace Survey and Earth Sciences (ITC), Enschede, The Netherlands are cooperating in a project to try to detect, monitor and measure the coal fires using remotely sensed data.
This paper describes the project's current status. The first main element of the study is the development of a fire detection and monitoring system based on the synergistic use of different remote sensing data sets. The usefulness of the various types of data is assessed and the difficulties in detecting the thermal anomalies produced by the coal fires are described. The other main aim of the project is to find a way to quantify the fires: that is, to try and determine their depth, temperature and extent. This requires modelling of the heat flow in the vicinity of the fires and the models which are being used for this purpose are discussed.

KURZFASSUNG

Unterirdische Kohlefeuer sind ein ernsthaftes Problem in vielen Gebieten der Welt, aber die wohl problematischste Erscheinung dieser Feuer bietet sich zur Zeit in China. Kohlefeuer treten hauptsächlich im Norden des Landes auf und haben eine Ausbreitung von 5000 km in Ost-West-Richtung und 450 km in Nord-Süd-Richtung. Die Probleme, die durch diese Feuer entstehen, schließen sowohl den Verlust des wertvollen wirtschaftlichen Rohstoffs, die Gefahr für Minenarbeiter und -ausrüstung als auch eine ernstzunehmende Umweltverschmutzung im lokalen und globalen Maßstab ein.
Enorme Anstrengungen zur Feuerbekämpfung werden durch das chinesische Ministerium für Kohleindustrie unternommen. Dennoch wird dessen Arbeit durch die Unzugänglichkeit der Feuer desöfteren erschwert. Deswegen arbeiten die Aerophotogrammetry and Remote Sensing Corporation of China Coal (ARSC) und das International Institute for Aerospace Survey and Earth Sciences (ITC), Enschede, Niederlande, in einem Projekt zusammen mit dem Ziel, die Kohlefeuer mit Hilfe von Fernerkundungsdaten erst zu entdecken, dann zu beobachten und später zu messen.
Dieser Artikel beschreibt den momentanen Stand des Projekts. Der erste Teil der Studie ist die Entwicklung eines Systems zur Feuerentdeckung und -beobachtung basierend auf der kombinierten Nutzung verschiedener Fernerkundungsdatensätze. Der Nutzen der verschiedenen Datensätze wird abgeschätzt, und die Schwierigkeiten beim Erfassen von thermischen Anomalien hinsichtlich der Kohlefeuer werden beschrieben. Ein anderes Hauptanliegen des Projekts liegt in der Erfassung der Feuer, d.h. die Bestimmung ihrer Tiefe, Temperatur und Ausdehnung. Hierzu muß der Wärmestrom der Umgebung der Feuer modellieret werden. Die für diesen Zweck benutzen Modelle werden näher erläutert.

1. COAL FIRE DETECTION

1.1 Review

Several attempts to detect underground coal fires using thermal remotely sensed data have been described in the literature (e.g. Bhattacharya et al., 1996; Mansor et al., 1994). Data from both satellite and airborne sensors were used with some success for the detection of known fires. The fires were detectable simply because of the heat which conducted from the fires to the surface, producing surface temperature anomalies (Greene et al., 1969). Sometimes, convection of heat through cracks and fissures in the rock led to smaller, hotter thermal anomalies (Ellyett and Fleming, 1974).

Most coal fires are thought to be caused by spontaneous combustion - a natural process. This, of course, means that oxygen must be able to reach the coal and we have evidence from our own work that many fires begin at exposed coal outcrops. The fires can then spread along the coal seam to greater depths as long as there is still some oxygen supply. Although most of the fires are natural, there seems to be a tendency for more fires to occur in regions of mining activity (Bhattacharya et al., 1996). This is mainly because the opening up of mines increases the supply of oxygen to the coal and there is an increased risk of fires being started by accident or careless mining practices.
Although coal fires were once common in countries such as the United States 'and the United Kingdom (Slavecki, 1965), nowadays it is India and, in particular, China, the world's largest coal producer, that experience the most severe coal fire problems.

The Chinese problem is vast; in fact, the amount of coal lost to fires there can only be guessed at (The loss was estimated to be between 100 and 200 million tonnes in 1992 (Rozema et al., 1995).) Particular problems in the case of the Chinese coal fires are the vast area over which the fires are spread and the remoteness of many of the areas in which they occur. This situation would seem to present a good opportunity for the use of remote sensing data for fire detection and monitoring. Obviously one would want to use data with as high as resolution as possible - probably airborne data - for this, but it would be impractical to gather such data for the whole of the fire-prone areas. For this reason, a hierarchical detection scheme is being tested, whereby thermal anomalies are first looked for in low resolution data and subsequently in data sets of higher and higher resolution. At each stage, the area investigated is smaller.
Images from the thermal bands of the NOAA-AVHRR, ERS-1-ATSR and Landsat-TM sensors have been acquired together with thermal data gathered by an airborne multispectral scanner belonging to the ARSC. It is also hoped to acquire some RESURS-01 data later.

1.2 Detection of Thermal Anomalies

In order to test the detection methods, three small test areas, known to contain active fires were chosen for detailed study. These test areas lay in north-western China, close to the city of Urumqi, the capital of Xinjiang Autonomous Region.
From a first look at the data available, it was obvious that the most clearly visible thermal anomalies were to be found in the airborne thermal scanner data. These data were therefore considered first, in contrast to the pattern of the intended final detection scheme. The first question to decide upon was how to define a temperature anomaly. Looking at the airborne data, there were clearly defined areas which would instinctively be considered as anomalously warm (see figure 2). It was decided to use this as a working definition; in fact, it was found that the pixels defined as being anomalous in this way closely matched the hottest 0.1% of pixels for all the airborne scenes.
The next problem was how to determine which of the thermal anomalies really were caused by coal fires. From fieldwork carried out in 1994, it was known that there were four possible causes of temperature anomalies within the study areas. These were: coal fires, solar heating of the ground, abnormal geothermal fluxes and human activities. The effect of abnormal geothermal fluxes was known to be very small and could therefore be neglected. Heat sources such as power stations and steel works have well-known positions. That left solar heating of the ground as the most likely source of temperature anomalies that could be confused with coal fires.
The positions of the thermal anomalies detected using the airborne thermal data were compared with digitised geological maps of the test areas. All thermal anomalies that lay within the coal-bearing rock strata were considered to be caused by coal fires. However, there were far fewer clearly visible thermal anomalies in the day-time images than in the night-time images - compare figure 3 with figure 2. The distribution of thermal anomalies in the night-time data corresponded closely to the positions of fires known from fieldwork. It was considered that it was the (uneven) solar heating of the test area that made the day-time data less suitable for detecting the coal fire thermal anomalies.
The day-time TM imagery was also affected by solar heating. Figures 4 and 5 are day- and night-time band 6 images, respectively, of the Kelazha test area south-west of Urumqi. The night-time image was acquired on 7th April 1995 and the day-time image on 14th September 1994. Two anomalously warm areas can be seen in the day-time image: the long white belt near the top and the curved feature near the centre. The first anomaly could not be detected in the night-time image and its appearance in the day-time scene was assumed to be due to solar heating. From its position and form, it was reasonable to think that the other anomaly corresponded to the fire already detected in the airborne imagery. Because of the lower spatial resolution of the TM data, there is less detail visible in these images than in the corresponding airborne images.
An attempt was made to remove some of the solar heating effects by producing a relative solar illumination map of the Kelazha area. This was done with the aid of a slope map, derived from a digital elevation model, and calculations of the solar position at the time of image acquisition. The solar illumination map (values 0-255) was subtracted from the original TM image. Figure 6 shows the result of adjusting the 7th April 1995 image in this way. It can be seen that most of the thermal anomalies in the top image are suppressed but that the others remain. The distribution of thermal anomalies now corresponds more closely to that of the night-time TM and night-time airborne images.
As yet, no coal fires have been detected using the AVHRR data and we are now fairly sure that none will be. This is not surprising given the low spatial resolution of these data. Work on the ATSR images is in progress. The RESURS-01 data still have to be acquired.

2. THERMAL MODELLING OF COAL FIRES

2.1 Soil Temperature Determination

The methods described so far can successfully locate many coal fires approximately. In addition, successful fire-fighting needs as much information as possible regarding the depth, temperature and extent of the fires.
Several of the fire detection studies mentioned earlier in this paper included descriptions of attempts to determine either the depth or temperature of an underground fire. One of these quantities was known, or estimated; the other was then calculated using some form of heat conduction equation. With the exception of a study of coal fires in the Jharia coalfield, India (Prakash et al., 1995), no-one has successfully determined both the depth and temperature of an underground fire from surface information alone, and even in the Jharia study an estimate of the fire's age was needed. The second major part of this research concerns the development of thermal models that will allow the depth, temperature and size of underground fires to be determined using only information obtainable at the surface.
It is well known that the temperature of an outdoor surface depends on many factors: the time of day and of the year, the weather conditions, slope, aspect, type of surface, etc. (Sabins, 1987). This means that the temperature of the ground above the coal fires is not affected by the fires alone, as was clearly demonstrated by the difficulty in detecting the fires using day-time images. For this reason, it was thought that it would be easier to begin the thermal modelling using data that were free of these surface effects.
Close to the surface, soil temperatures follow an approximately sinusoidal temperature curve on both a diurnal and an annual cycle (Jury et al., 1991). The amplitude of these temperature waves decreases with increasing depth until at a certain depth, the variations cease. It is observed that the annual temperature

variation, which is generally larger, penetrates to greater depths than the diurnal wave. These depths vary but are usually of the order of tens of centimetres for the diurnal wave and a few metres for the annual wave. It was decided that temperature data from just below the surface should be gathered for selected fires to allow the thermal models to be developed and tested. This was made one of the main aims of the field campaign in the Xinjiang test areas carried out in August and September of 1995.

2.2 Field Temperature Measurements

The first important task was to determine the depth to which the diurnal temperature variations penetrated in the test area soil. Two of the fires in the Kelazha area were chosen for particular study. A portable weather station was then set up about 1 km from the nearest fire. The weather station included equipment for making soil temperature measurements and we first wanted data that were not influenced by the fires. Soil temperatures were gathered at depths of 2, 4, 8, 16, 32 and 64 cm for a period of about four-and-a-half days. Measurements were made every ten minutes and were stored using a data logger. It was observed that there was virtually no temperature variation at a depth of 64 cm throughout the measurement period and there was only a very slight variation at 32 cm. At the shallower depths the temperature wave was more significant. This suggested that soil temperature measurements made at depths of more than about 30 cm, in a similar soil, would be almost unaffected by the diurnal temperature variation. It was more important to consider the diurnal rather than the annual temperature variation at this stage because only the diurnal temperature variation would produce a significant change in temperature over the measurement period.

Measurement grids were marked out at the two coal fires. The sites were obviously close to active fires - smoke and sulphurous deposits on the ground were clearly visible - and rough surveys of surface temperatures had been made with a hand-held radiometer to determine the approximate location of the associated thermal anomalies. At the first fire, known as fire 141, the grid measured 30 m by 30 m; at the second fire, fire 143, 15 m by 15 m. Temperature measurements at depths of 30 and 50 cm were made every 5 m at fire 141 and every 3 m at fire 143. The size of the grids was limited by the extent of the areas that had fairly constant slope and soil characteristics. The temperature measurements were made at two depths so that the temperature gradient at each point could be estimated. As discussed above, 30 cm was about the minimum depth that the measurements could be made at. It would have been preferable to measure at slightly greater depths but this was not practical because of the hard ground.

2.3 Dip Angle Model

Several authors of coal fire studies (e.g. Mukherjee et al., 1991, Bhattacharya and Reddy, 1994) have made use of the equation of linear heat flow in a semi-infinite medium (Carslaw and Jaeger, 1959) for estimating either the depth or temperature of an underground fire. Knowing, or estimating one of these quantities allowed the other to be calculated. In their study, Saraf et al. (Saraf et al., 1995) calculated the depth of a fire by assuming that the fire lay directly below the observed surface temperature anomaly, measuring the distance of this anomaly to the nearby coal outcrop and measuring the dip angle of the coal seam. The depth of the coal, and of the fire, followed from simple trigonometry.

For both Kelazha test sites, the distance of the nearest coal outcrop to the corner of the test grids was measured and the dip of the appropriate coal layer was estimated through general observations of the area's geology. (The rocks were well-exposed in this semi-desert area.) This allowed an estimate of the depth of the coal below each measurement point to be made.

The equation of linear heat flow really applies to non steady-state conditions and requires an estimate of the age of the heat source. We assumed, instead, that steady-state heat conditions were applicable and made use of our temperature gradient measurements.

The 'raw' temperature gradients measured at the two fires were corrected for the influence of the solar heat flux using the weather station data, to give an estimate of the true vertical heat flux due to the fires. Multiplying the temperature gradients by the appropriate coal depths and adding them to the observed temperatures produced corresponding grids of supposed 'fire temperatures', directly below each grid point.

For both fires, the calculated temperatures were far above what would be expected for burning coal. Coal burns at temperatures of up to around 2000 °C (ARSC, 1989); the calculated temperatures were of the order of several thousand degrees. The reason for the discrepancy was probably that this model was too simple and made too many assumptions. The heat flow was assumed to be one-dimensional only, the medium through which the heat flowed homogeneous and the coal seam dip constant with depth. In addition, many cracks through which hot gases were escaping were observed, suggesting that a considerable amount of heat was being transferred to the surface by convection rather than conduction. The results suggest that this 'dip angle' model is not a suitable approach to the modelling of these fires.

2.4 Radial Heat Flow Model

A more sophisticated approach was developed based on the following idea. For one (near) surface temperature measurement, there is an infinite range of possible distances to the fire from this point and of fire temperatures. However, the grids of temperature measurements made in the field constrain the number of possible solutions; they are, in fact, boundary, conditions.

For the case of spherically symmetric heat flow around a point heat source, the total heat flow, H, across any surface surrounding the heat source is given by

$$H = -k4\pi r^2 \frac{dT}{dr} \qquad \text{(Equation 1)}$$

where k is the thermal conductivity, T is the temperature and r is the distance from the heat source. This leads to the results (Sears et al., 1982)

$$H = \frac{4\pi kab\,(T_2 - T_1)}{b - a} \qquad \text{(Equation 2)}$$

and

$$T = T_2 - \frac{b\,(r - a)\,(T_2 - T_1)}{r\,(b - a)} \qquad \text{(Equation 3)}$$

where a, b and r are as shown in fig. 1. T is the temperature at distance r from the centre, T_2 the temperature at distance a, and T_1 the temperature at distance b.

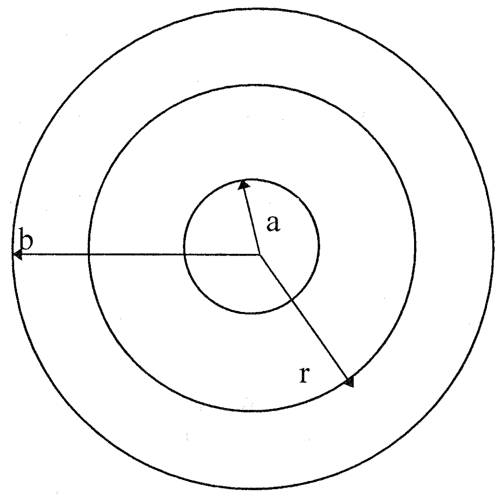

Figure 1. Basis of radial heat flow model

These results can be used in the following way. Take one of the measured temperatures and assume it is 'correct'; i.e., it would fit equations 2 and 3 exactly if all the other quantities were known. Then, for a range of values of fire temperature (at radius a), position and radius, calculate the implied temperature at the other grid points. (If the fire position is defined relative to one grid point the distances to all the other points follow.) The set of values of fire position, radius and temperature which produces the best match between calculated and measured temperatures is the solution to the problem.
A FORTRAN program was written to perform these calculations. The following 'space' was searched for solutions in the case of fire 141

x co-ordinate : -100 to 100 m with resolution 2m
y co-ordinate : -100 to 100 m with resolution 2m
z co-ordinate : -100 to 100 m with resolution 2m
temperature: 750 to 2500 K with resolution 50 K
fire radius: 2 to 30 m with resolution 2 m

and for fire 143 solutions in the intervals

x co-ordinate : -250 to 250 m with resolution 10 m
y co-ordinate: -250 to 250 m with resolution 10 m
z co-ordinate: -200 to 200 m with resolution 10 m
temperature: 500 to 2500 K with resolution 100 K
fire radius: 2 to 30 m with resolution 2 m

The 'top left' corner of the measurement grid was assigned the co-ordinates (0, 0, 0) in both cases. Positive z co-ordinates (above the level of the origin) were tried as solutions because of the hilly relief in the test areas. It would be quite possible to have an underground fire above the level of the measurement grid.

2.5 Radial Model Results

The results of applying this model were rather better for fire 141 than for fire 143. The best solution found in the case of fire 141 was for a fire with a temperature of 1050 K and radius 2 m centred at co-ordinates (22, 26, 0). The average difference between calculated and observed temperatures was then 7.65 K per grid point. The important point is that all the other 'good' solutions had very similar 'co-ordinates'. No other region of solutions was found even with the quite fine intervals used. The solution was, therefore, well-defined. With a five-dimensional space to search, the intervals used were about the finest practical.
The best solutions for fire 143 did not match the observed temperatures as closely; the best solution had an average error of 11.84 K. The problem was that according to this solution, the temperatures at 30 cm would then be higher than those at 50 cm, the opposite of what was observed. It could be that the solar heat flux penetrated to greater depths at this test site because of a difference in soil properties and that this affected the results.
The results for fire 141, which at first sight look encouraging, have to be carefully interpreted. What the solutions actually imply is that an object of a particular radius with a particular surface temperature would produce certain temperature patterns at the surface - in some cases very similar to the observed temperatures. This is not the same as saying that the fires definitely have these radii and temperatures even if the model is correct, because this model does not apply to the region in which the heat is generated. It might be possible to model the temperature distribution within this region if an 'edge of fire' temperature could be defined, but this is difficult. The main usefulness of the model, in fact, is in determining the fire position. Equation 2 could also be used to estimate the total heat flux form the fire if the thermal conductivity of the rocks were known. This could then be converted to a rate of coal burning, which is another thing we wish to know.
The other main limitation of this model is that it can only really deal with situations of constant thermal conductivity. In the field, there could be many different rock types present between the fire and the area where temperature measurements are made. It would not be practical to apply analytical techniques in this situation. A numerical technique, such as the finite element method, is required for this. The ANSYS® finite element software has recently been acquired and is now being used for this purpose.

3. CONCLUSIONS AND FUTURE WORK

A coal fire detection system based on Landsat-TM and airborne data, at least, seems feasible. The TM data can be used to detect larger fires and to map areas worthy of more detailed investigation using airborne data. Care has to be taken to remove solar heating effects from day-time data. It would be preferable to always use night-time 'pre-dawn' data for detection but these can be difficult to acquire, especially in the case of TM.
The radial heat flow model could be useful for determining fire locations. It and the anticipated numerical model require further testing. This should be possible after a further field campaign this summer. It is planned then to repeat the soil temperature measurements at sites in Ningxia province and the data gathered will be used as inputs to the models. The difference is that, for the Ningxia fires, extensive borehole temperature data down to the fires exist; everything we want to model is in effect already known. The models' usefulness will be assessed by comparing the new results with these temperature data.
The other major piece of work still to be carried out is to find a way of 'correcting' the surface temperatures determined from the remote sensing data for the influence of the temperature variations described earlier. This would remove the need for sub-surface temperature measurements. The solar heating maps are not

sufficient for this purpose; they only make a relative estimate of the amount of solar radiation reaching the ground. The influences on the surface temperature are much more complex. Only the airborne data are of sufficient resolution for fire modelling but if a way could be found to use these data directly in the thermal models, it would be possible to construct approximate models, at least, for many more fires. We would then have a complete remote sensing-based coal fire detection and measurement system.

ACKNOWLEDGEMENTS

The authors would like to thank members of the ARSC and of the Institute of Physical Geography, University of Freiburg, Germany for their assistance, particularly with the fieldwork.
This research is funded by the European Commission under contract nos. P2034552 and P2036005.

REFERENCES

ARSC, 1989. Delineation of the burnt rock in Xinmin area, Shenfu coal field, China. Internal Report, p.25. (In Chinese)

Bhattacharya A. and Reddy, C. S. S., 1994. Underground and surface coal mine fire detection in India's Jharia coalfield using airborne thermal infrared data. Asian-Pacific Remote Sensing Journal, 7(1), pp. 59-73.

Bhattacharya, A., Reddy, C.S.S. and Manoj Dangwal, 1996. Coal mine fire inventory and monitoring in Jharia coalfield, Bihar, India, using thematic mapper thermal IR data. Proceedings of the Eleventh Thematic Conference and Workshops on Applied Geologic Remote Sensing, Las Vegas, USA, 27-29 February 1996.

Carslaw, H.W. and Jaeger, J.C., 1959. Conduction of Heat in Solids, 2nd edition. Clarendon Press, Oxford, p. 60.

Ellyett, C.D. and Fleming, A.W., 1974. Thermal infrared imagery of the Burning Mountain coal fire. Remote Sensing of the Environment, 3, pp. 79-86.

Greene, G.W., Moxham, R.M. and Harvey, A.H., 1969. Aerial infrared surveys and borehole temperature measurements of coal mine fires in Pennsylvania. Proceedings of 6th Symposium on Remote Sensing of the Environment, pp. 517-525. Published by University of Michigan, Ann Arbor, Michigan.

Jury, W.A., Gardner, W.R., Wilford., R. and Gardner, W.H., 1991. Soil Physics, 5th edition. John Wiley & Sons, New York, pp. 185-192.

Mansor, S.B., Cracknell, A.P., Shilin, B.V. and Gornyi, V.I., 1994. Monitoring of underground coal fires using thermal infrared data. International Journal of Remote Sensing, 15(8), pp. 1675-1685.

Mukherjee, T., Bandyopadhyay, T.K. and Pande S.K., 1991. Detection and delineation of depth of subsurface coalmine fires based on an airborne multispectral scanner survey in a part of the Jharia coalfield, India. Photogrammetric Engineering and Remote Sensing, 57(9), pp. 1203-1207.

Prakash, A., Sastry, R.G.S., Gupta, R.P. and Saraf A.K., 1995. Estimating the depth of buried hot features from thermal infrared remote sensing data: a conceptual approach. International Journal of Remote Sensing, 16(13), pp. 2503-2510.

Rozema, A., van Genderen, J.L. and Schalke, H.J.W.G., Beijing Remote Sensing Corporation, 1995. Environmental monitoring of coal fires in North China. Project Identification Mission Report, October 1993. Netherlands Remote Sensing Board (BCRS) Report 93-29, p.4.

Sabins, F.F., 1987. Remote Sensing Principles and Interpretation, 2nd edition. W.H. Freeman & Co., New York, pp. 133-135.

Saraf, A.K., Prakash, A., Sengupta, S. and Gupta, R.P., 1995. Landsat-TM data for estimating ground temperature and depth of subsurface coal fire in Jharia coalfield, India.

Sears, F.W., Zemansky, M.W. and Young, H.D., 1982. University Physics, 6th edition. Addison-Wesley, p.318.

Slavecki, 1965. Detection and location of subsurface coal fires. Proceedings of 3rd Symposium on Remote Sensing of the Environment, pp. 537-543. Published by University of Michigan, Ann Arbor, Michigan.

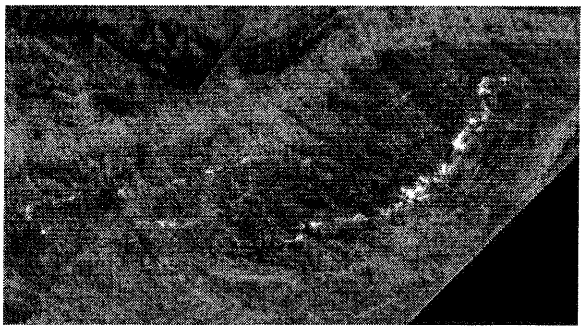

Figure 2. Night-time airborne thermal infrared scanner image of Kelazha area

Figure 5. Night-time TM band 6 image of Kelazha

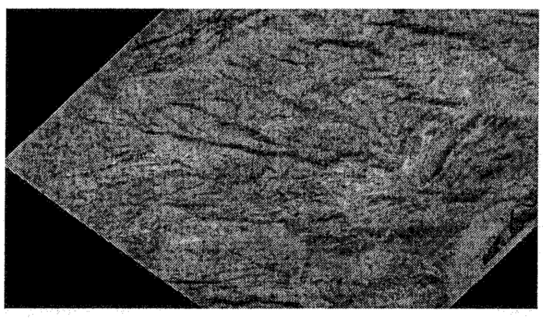

Figure 3. Day-time thermal thermal infrared scanner image of Kelazha area

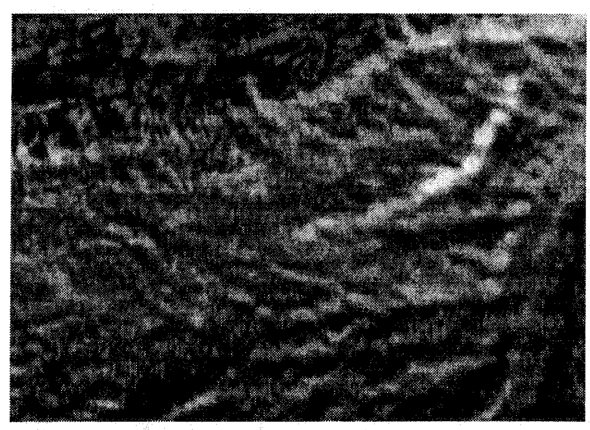

Figure 6. Day-time TM band 6 image adjusted for effects of solar heating

Figure 4. Day-time TM band 6 image of Kelazha